

Nonlinear Models for Double-Wall Systems for Vibrations and Noise Control

Yen Wei* and Rimas Vaicaitis†
Columbia University, New York, New York 10027

A theoretical model is developed for active control of vibrations and noise transmission of nonlinear double-wall systems to random wideband inputs. A velocity feedback control mechanism is integrated into governing nonlinear equations of motion using piezoelectric materials as sensors and actuators. The nonlinear von Kármán thin plate theory is used to model vibrations of the face plates. A soft elastic core of the double wall is used. The nonlinear panel response is obtained by utilizing modal analyses and Monte Carlo simulation techniques. Transmitted noise inside a rectangular enclosure is obtained by solving the linearized acoustic wave equation subject to time-dependent boundary conditions of the vibrating interior panel. Numerical results include vibration response time histories, spectral densities, rms responses, and noise reduction. The feasibility of using piezoelectric velocity feedback actuators for active control of nonlinear vibrations and noise transmission to random inputs is demonstrated.

Nomenclature

A, B	= dimensions of piezoelectric actuator in x and y directions, m
a, b, d	= cavity dimensions in x, y, z directions, m
c_T	= viscous damping coefficient of top plate, N-s/m ³
c_0	= speed of sound, m/s
D_T	= $E_T h_T^3 / 12(1 - \nu_T^2)$, top plate
d_{ij}	= piezoelectric strain charge constants, m/V
E_{PZT}	= modulus of elasticity of piezoelectric material, N/m ²
E_T, E_B	= moduli of elasticity at top and bottom plates, N/m ²
E_3	= electric field, V/m
F_T	= Airy stress function of top plate
h_{PZT}	= thickness of piezoelectric actuator, m
h_s	= thickness of the core, m
h_T, h_B	= thickness of top and bottom plates, m
K	= conversion gain factor, V-s/m
L_x, L_y	= dimensions of double-wall plate in x and y directions, m
m_{PZT}	= mass of the piezoelectric actuator, kg-s ² /m ³
m_s	= mass of the core, kg-s ² /m ³
m_T, m_B	= mass of top and bottom plates, kg-s ² /m ³
$P_T(x, y, t)$	= random input pressure, N/m ²
$p(x, y, z, t)$	= acoustic pressure, N/m ²
$S_p(x, y, z, \omega)$	= spectral density of acoustic pressure, (N/m ²) ² /rad/s
$S_p(\omega)$	= spectral density of input random pressure, (N/m ²) ² /rad/s
u, v, w	= displacements along x, y, z directions, m
$V(t)$	= feedback voltage, V
w_T, w_B	= normal displacements of top and bottom plates in z direction, m
ν	= Poisson's ratio
ν_T, ν_B, ν_{PZT}	= Poisson's ratios of top and bottom plates and piezoelectric actuator

ξ_{nm}	= structural modal damping coefficients
ρ_a	= air density, kg-s ² /m ⁴
ρ_s	= material density of the core, kg-s ² /m ⁴
ρ_T, ρ_B	= material density of top and bottom plates, kg-s ² /m ⁴
Φ_{ijk}	= acoustic modal damping coefficients
Ω_T	= location function of piezoelectric sensors/actuators
ω	= frequency, rad/s
ω_{ijk}	= acoustic modal frequencies, rad/s
ω_{nm}	= structural modal frequencies, rad/s

Introduction

STRUCTURAL dynamic response and noise transmission of surface protection systems are important factors in the design and safety of modern high-speed flight vehicles, operation and reliability of highly sensitive electronic equipment, stealthiness characteristics, and aerodynamic efficiency. With increasing use of lightweight materials, problems of fatigue, degradation of strength, and high levels of transmitted and radiated noise can be expected for severe aerodynamic, acoustic, and thermal environments.^{1–3} It has been demonstrated that vibrations of surface panels are often nonlinear and response statistics are no longer Gaussian.^{4–9} Thus, it is necessary to develop methods for the control of nonlinear vibrations and noise transmission to random wideband inputs.

Advances in control theory, high-speed processors, and fast-growing development of various kinds of smart materials have made it possible to develop active control procedures for noise and vibration reduction.^{10–20} Materials that have been investigated for the application of active control of vibrations and noise include: optic fibers,²¹ piezoelectric polymers and ceramics,^{11–15} shape memory alloys,^{22,23} electrostriction,²⁴ magnetostriction,²⁵ electrorheological fluids,²⁶ etc. At the present time, piezoelectric polymers and ceramics have been recognized as providing the most favorable mechanisms for practical implementation. Among the widely used procedures for active control are velocity feedback,^{11,13,14} mean square sound energy minimization,^{15–18} sound pressure feedback,¹⁸ and modal rearrangement.^{19,20} Most of these studies are limited to deterministic inputs and linear structural and acoustic systems. An analytical study of active control of nonlinear response and noise transmission into a rectangular enclosure of a double-wall sandwich system is presented in this paper.

Following the von Kármán thin plate theory and electro-mechanical equations of piezoelectricity,^{27,28} the governing

Received March 16, 1996; revision received June 1, 1997; accepted for publication July 5, 1997. Copyright © 1997 by the American Institute of Aeronautics and Astronautics, Inc. All rights reserved.

*Postgraduate Student, Department of Civil Engineering and Engineering Mechanics.

†Professor, Department of Civil Engineering and Engineering Mechanics. Associate Fellow AIAA.

equations of motion with velocity feedback control of nonlinear vibrations of a double-wall construction are developed. Linear and nonlinear uniaxial spring–dashpot models are chosen to characterize behavior of the soft core where bending and shearing stresses are neglected. The boundary conditions of the face plates are assumed to be simple supports on all edges. The piezoelectric sensors/actuators are bonded symmetrically to both sides of each face plate. The input acting on the external (top) face plate is taken to be uniformly distributed stationary and Gaussian random pressure. The time-history realizations of input pressure are generated by the simulation procedures of stationary random processes.²⁹ A modal analysis is utilized to decompose the vibrations of the face plates and the coupled system is solved by a Galerkin-like procedure and numerical integration in time domain.^{30,31} In this approach, it is assumed that the effect of external radiated and cavity-transmitted acoustic pressure on structural response can be neglected.

The transmitted noise inside a rectangular enclosure is obtained by solving the acoustic wave equations subject to time-dependent boundary conditions of the vibrating interior (bottom) face plate. To obtain a fast and uniformly converging solution for the interior acoustic pressure, the homogeneous acoustic equation with nonhomogeneous boundary conditions is transformed into a nonhomogeneous equation with homogeneous boundary conditions using Green's theorem. The required vibration response spectral densities of the bottom plate are obtained by taking a fast Fourier transform (FFT) of the nonlinear response time histories.

This paper includes numerical results of nonlinear vibration response time histories, rms responses, spectral densities, and noise reduction for actively controlled and noncontrolled cases. The interactions between the controlled variables and the effect on vibration and noise transmission is investigated. These include size, location, and number of piezoelectric actuators and arrangement of actuators on both face plates.

Problem Formulation and Solution of Nonlinear Response of a Double-Wall System

The problem geometry and basic features of active control mechanisms are shown in Fig. 1. The double-wall system is composed of a soft core and two elastic face plates. The piezoelectric sensors/actuators are symmetrically bonded to the plates as shown in Fig. 2. The top and bottom plates are simply supported on all four edges. Because of the similarity of the coupled equations of the top and bottom plates, equations of motion are first developed for the top plate. Following the von Kármán nonlinear plate theory and assuming that each piezoelectric actuator is a thin slab of ferroelastic material poled in the z direction, the equations of motion in the form of stress resultants are^{5,27,28}

$$\begin{aligned} & \frac{\partial^2 M_x^T}{\partial x^2} + 2 \frac{\partial^2 M_{xy}^T}{\partial x \partial y} + \frac{\partial^2 M_y^T}{\partial y^2} + N_x^T \frac{\partial^2 w_T}{\partial x^2} + 2 N_{xy}^T \frac{\partial^2 w_T}{\partial x \partial y} + N_y^T \frac{\partial^2 w_T}{\partial y^2} \\ & - c_T \dot{w}_T - K_S(w_T, w_B) - m_s \left(\frac{1}{3} \ddot{w}_T + \frac{1}{6} \ddot{w}_B \right) \\ & - 2 \Omega_T \left[m_{PZT} \ddot{w}_T - \rho_s h_{PZT} \left(\frac{1}{3} \ddot{w}_T + \frac{1}{6} \ddot{w}_B \right) \right] \\ & + P_T(x, y, t) = m_T \ddot{w}_T \end{aligned} \quad (1)$$

where

$$[M_x^T, M_y^T, M_{xy}^T] = \int_{-\lambda}^{\lambda} [T_1^T, T_2^T, T_6^T] z \, dz \quad (2)$$

$$[N_x^T, N_y^T, N_{xy}^T] = \int_{-\lambda}^{\lambda} [T_1^T, T_2^T, T_6^T] \, dz \quad (3)$$

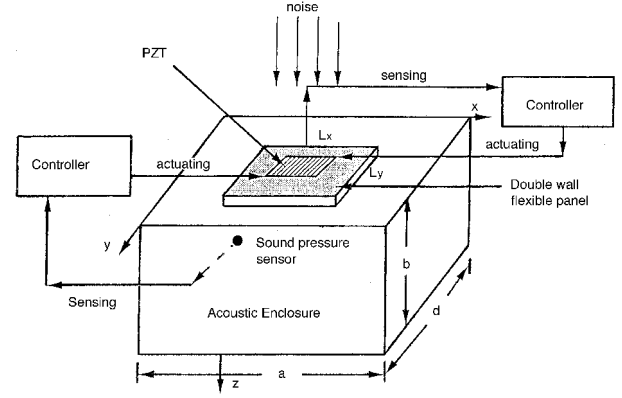


Fig. 1 Active vibration and noise transmission control mechanism of a double panel system.

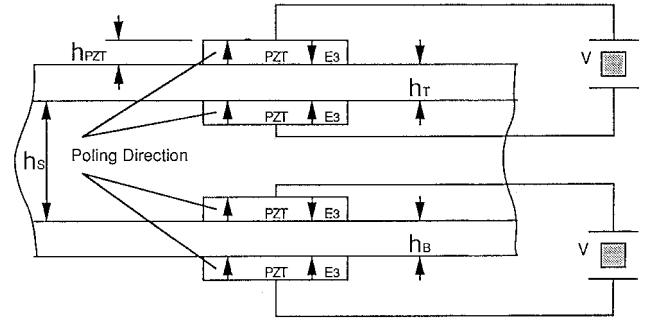


Fig. 2 Bonding of PZT to top and bottom plates.

$$\begin{bmatrix} T_1^T \\ T_2^T \\ T_6^T \end{bmatrix} = [c_{PZT}]([\theta_0] + z[\kappa] + [\theta_N]) - [c_{PZT}] \begin{bmatrix} d_{31} E_3 \\ d_{32} E_3 \\ 0 \end{bmatrix} \quad (4)$$

The $[c_{PZT}]$ matrix is given in the Appendix. The limits of integration in Eqs. (2) and (3) are $\lambda = h_T + \Omega_T h_{PZT}$. The location function $\Omega_T(x, y)$ denotes the presence of a piezoelectric actuator and is defined as $\Omega_T(x, y) = 1$, where the actuator is bonded to the plate and $\Omega_T(x, y) = 0$, otherwise. The $K_S[w_T, w_B]$ is the constitutive linear/nonlinear law operator of the soft core, and $P_T(x, y, t)$ is the external random pressure that could represent powerplant exhaust noise, turbulent boundary-layer noise, impinging shock loading, and other external disturbances that might be acting on the surface thermal protection systems. The inertia force of the soft core is assumed to vary linearly where the terms $m_s/3$ and $m_s/6$ in Eq. (1) are applied contributions of the mass of the soft core to the two face plates. The linear strain, curvature, and nonlinear contributions in Eq. (4) are

$$\begin{aligned} [\theta_0] &= \begin{bmatrix} \frac{\partial u}{\partial x} \\ \frac{\partial v}{\partial y} \\ \frac{1}{2} \left(\frac{\partial u}{\partial y} + \frac{\partial v}{\partial x} \right) \end{bmatrix}, \quad [\kappa] = \begin{bmatrix} \frac{\partial^2 w}{\partial x^2} \\ -\frac{\partial^2 w}{\partial y^2} \\ -\frac{\partial^2 w}{\partial x \partial y} \end{bmatrix} \end{aligned} \quad (5)$$

$$\begin{aligned} [\theta_N] &= \begin{bmatrix} \frac{1}{2} \left(\frac{\partial w}{\partial x} \right)^2 \\ \frac{1}{2} \left(\frac{\partial w}{\partial y} \right)^2 \\ \frac{1}{2} \frac{\partial w}{\partial x} \frac{\partial w}{\partial y} \end{bmatrix} \end{aligned}$$

The piezoelectric constants d_{ij} of a material poled in the z direction are given in Ref. 32. The electric field E_3 can be related to applied voltage V , by $V = E_3 h_{\text{PZT}}$.

Substituting Eqs. (2–5) into Eq. (1) and defining membrane in-plane forces as

$$N_x^T = \frac{\partial^2 F_T}{\partial y^2}, \quad N_y^T = \frac{\partial^2 F_T}{\partial x^2}, \quad N_{xy}^T = -\frac{\partial^2 F_T}{\partial x \partial y} \quad (6)$$

where F_T is the Airy stress function, gives the electromechanical equations of the top plate

$$\begin{aligned} m_T \ddot{w}_T + c_T \dot{w}_T + D_T \nabla^4 w_T - \frac{\partial^2 F_T}{\partial y^2} \frac{\partial^2 w_T}{\partial x^2} + 2 \frac{\partial^2 F_T}{\partial x \partial y} \frac{\partial^2 w_T}{\partial x \partial y} \\ - \frac{\partial^2 F_T}{\partial x^2} \frac{\partial^2 w_T}{\partial y^2} + K_S [w_T, w_B] + m_S \left(\frac{1}{3} \ddot{w}_T + \frac{1}{6} \ddot{w}_B \right) \\ + 2\Omega_T \left[m_{\text{PZT}} \ddot{w}_T - \rho_S h_{\text{PZT}} \left(\frac{1}{3} \ddot{w}_T + \frac{1}{6} \ddot{w}_B \right) \right] \\ + D_T \alpha \frac{E_{\text{PZT}}}{E} \left\{ \frac{\partial^2}{\partial x^2} \left[\Omega_T \left(\frac{\partial^2 w_T}{\partial x^2} + \nu_{\text{PZT}} \frac{\partial^2 w_T}{\partial y^2} \right) \right] \right. \\ \left. + \frac{\partial^2}{\partial y^2} \left[\Omega_T \left(\nu_{\text{PZT}} \frac{\partial^2 w_T}{\partial x^2} + \frac{\partial^2 w_T}{\partial y^2} \right) \right] \right. \\ \left. + 2(1 - \nu_{\text{PZT}}) \frac{\partial^2}{\partial x \partial y} \left[\Omega_T \frac{\partial^2 w_T}{\partial x \partial y} \right] \right\} = P_T(x, y, t) \\ - \frac{1}{1 - \nu_{\text{PZT}}} [(h_T + h_{\text{PZT}}) E_{\text{PZT}} d_{31} V(t) \nabla^2 \Omega_T] \end{aligned} \quad (7)$$

here $\alpha = 6\beta + 12\beta^2 + 8\beta^3$ and $\beta = h_{\text{PZT}}/h_T$. In obtaining Eq. (7), it was assumed that the piezoelectric material bonded to the plate surface does not extend to the edges of the plate. The compatibility equation in terms of the Airy stress function is^{5,27}

$$\nabla^4 F_T = E_T h_T \left[\left(\frac{\partial^2 w_T}{\partial x \partial y} \right)^2 - \frac{\partial^2 w_T}{\partial x^2} \frac{\partial^2 w_T}{\partial y^2} \right] \quad (8)$$

Similar sets of equations can be developed for the bottom plate of the double-wall construction by interchanging subscripts T and B , adjusting loading conditions and apportioned mass of the core corresponding to those of the bottom plate.

The boundary conditions corresponding to vertical deflections w_T and w_B are those of simply supported plates. Exact boundary conditions for the Airy stress function are very complicated. In the present study, in-plane boundary conditions are satisfied on the average³⁰

$$\int_0^{L_y} \int_0^{L_x} \frac{\partial u}{\partial x} dx dy = 0, \quad \int_0^{L_y} \int_0^{L_x} \frac{\partial v}{\partial y} dx dy = 0 \quad (9)$$

$$\left[\frac{1}{L_y} \int_0^{L_y} N_{xy} dy \right] \Big|_{x=0, L_x} = 0, \quad \left[\frac{1}{L_x} \int_0^{L_x} N_{yx} dx \right] \Big|_{y=0, L_y} = 0 \quad (10)$$

The subscripts T and B in the preceding and next equations are dropped for brevity. The in-plane displacements u and v are related to the stress function F as

$$\frac{\partial u}{\partial x} = \frac{1}{Eh} \left(\frac{\partial^2 F}{\partial y^2} - \nu \frac{\partial^2 F}{\partial x^2} \right) - \frac{1}{2} \left(\frac{\partial w}{\partial x} \right)^2 \quad (11)$$

$$\frac{\partial v}{\partial y} = \frac{1}{Eh} \left(\frac{\partial^2 F}{\partial x^2} - \nu \frac{\partial^2 F}{\partial y^2} \right) - \frac{1}{2} \left(\frac{\partial w}{\partial y} \right)^2 \quad (12)$$

The first two conditions given in Eq. (9) imply no in-plane stretching of the plane midsurface, while the last two specify vanishing in-plane shear at the plate boundaries.

The complexity of the nonlinear Eqs. (7) and (8) prompts us to find an approximate solution. The vertical deflections of the top and bottom plates are expressed in the form of functions $X_{nm}(x, y)$, which satisfy all the boundary conditions for normal deflections^{30,31}

$$w_T(x, y, t) = \sum_{n=1}^N \sum_{m=1}^N A_{nm}^T(t) X_{nm}(x, y) \quad (13)$$

$$w_B(x, y, t) = \sum_{n=1}^N \sum_{m=1}^N A_{nm}^B(t) X_{nm}(x, y) \quad (14)$$

where A_{nm}^T and A_{nm}^B are the generalized coordinates of the top and bottom plates, and $X_{nm} = \sin(m\pi x/L_x) \sin(n\pi y/L_y)$ for simply supported edges. The details on the validity and limitations of the approximate solutions expressed in the form of Eqs. (13) and (14) can be found in Refs. 30 and 31.

Substituting the series solution of Eq. (13) into the right-hand side of Eq. (8) results in a linear equation with respect to the stress function $F_T(x, y, t)$. The general solution for F_T will contain arbitrary functions, by means of which the boundary conditions for F_T can be satisfied.^{30,31} The solution for the stress function is expressed in approximate form

$$F_T = F_T^P + F_T^h \quad (15)$$

where F_T^P is a particular solution of Eq. (8), and F_T^h denotes a homogeneous solution of which the parameters are chosen in such a way that the conditions for $F_T(x, y, t)$ are satisfied on the average.³⁰ These solutions are of similar form as given in Refs. 5, 6, and 8. Following the same procedure, solutions for the Airy stress function for the bottom plate F_B can be developed.

Before the complete solutions to Eq. (1) can be developed, the constitutive operator $K_S[w_T, w_B]$ for the soft core needs to be selected. In the present study, it is assumed that the core can be modeled by a combination of linear/nonlinear elastic springs and dampers:

$$\begin{aligned} K_S[w_T, w_B] = k_1(w_T - w_B) + k_2(w_T - w_B)^2 + k_3(w_T - w_B)^3 \\ + c_1(\dot{w}_T - \dot{w}_B) + c_2(\dot{w}_T - \dot{w}_B)^2 + c_3(\dot{w}_T - \dot{w}_B)^3 \end{aligned} \quad (16)$$

where k_1 , k_2 , and k_3 are elastic spring constants, and c_1 , c_2 , and c_3 are damping coefficients. Furthermore, the number and location of the piezoelectric actuators need to be specified. Numerical results were obtained for one, five, and nine actuators that were bonded to each of the top and bottom plates. Consider the case where only one piezoelectric actuator with dimensions $A \times B \times h_{\text{PZT}}$ is placed in the middle on both sides of the bottom and top plates. Using the solution for the Airy stress function F_T and Eq. (13), Eq. (7) is satisfied in a Galerkin sense. The resulting system of the nonlinear coupled differential equations for the top plate are

$$\begin{aligned} m_T \ddot{A}_{nm}^T + c_T \dot{A}_{nm}^T + \left[\left(\frac{m\pi}{L_x} \right)^2 + \left(\frac{n\pi}{L_y} \right)^2 \right]^2 D_T A_{nm}^T \\ + \frac{E_T h_T \pi^4}{8(1 - \nu_T^2)} A_{nm}^T \left[\left(\frac{m}{L_x} \right)^2 \sum_{kl} (A_{kl}^T)^2 \left(\frac{k^2}{L_x^2} + \nu_T \frac{l^2}{L_y^2} \right) \right. \\ \left. + \left(\frac{n}{L_y} \right)^2 \sum_{kl} (A_{kl}^T)^2 \left(\nu_T \frac{k^2}{L_x^2} + \frac{l^2}{L_y^2} \right) \right] \\ + E_T h_T \left(\frac{\pi}{2L_y} \right)^4 \sum_{ijklrs} A_{ij}^T A_{kl}^T A_{rs}^T Z_{nmijklrs} + \frac{m_S}{3} \ddot{A}_{nm}^T \\ + \frac{m_S}{6} \ddot{A}_{nm}^B + k_1(A_{nm}^T - A_{nm}^B) + k_2 \sum_{ijkl} (A_{ij}^T - A_{ij}^B)(A_{kl}^T \end{aligned}$$

$$\begin{aligned}
& -A_{kl}^B \bar{\alpha}(m, i, k) \bar{\alpha}(n, j, l) + \frac{k_3}{16} \sum_{ijklrs} (A_{ij}^T - A_{ij}^B)(A_{kl}^T - A_{kl}^B)(A_{rs}^T \\
& - A_{rs}^B) \bar{\gamma}(m, i, k, r) \bar{\gamma}(n, j, l, s) + c_1(A_{nm}^T - A_{nm}^B) + c_2 \sum_{ijkl} (A_{ij}^T \\
& - A_{ij}^B)(A_{kl}^T - A_{kl}^B) \bar{\alpha}(m, i, k) \bar{\alpha}(n, j, l) + \frac{c_3}{16} \sum_{ijklrs} (A_{ij}^T - A_{ij}^B)(A_{kl}^T \\
& - A_{kl}^B)(A_{rs}^T - A_{rs}^B) \bar{\gamma}(m, i, k, r) \bar{\gamma}(n, j, l, s) \\
& + \frac{4D_T \alpha E_{PZT}}{L_x L_y E_T} \sum_j \left\langle \Omega_T, \left[\frac{\partial^2 X_{nm}}{\partial x^2} \left(\frac{\partial^2 X_{ij}}{\partial x^2} + v_{PZT} \frac{\partial^2 X_{ij}}{\partial y^2} \right) \right] \right. \\
& + \left[\frac{\partial^2 X_{nm}}{\partial y^2} \left(v_{PZT} \frac{\partial^2 X_{ij}}{\partial x^2} + \frac{\partial^2 X_{ij}}{\partial y^2} \right) \right] \\
& + \left. \left[2(1 - v_{PZT}) \left(\frac{\partial^2 X_{ij}}{\partial x \partial y} \frac{\partial^2 X_{ij}}{\partial x \partial y} \right) \right] \right\rangle A_{ij}^T \\
& = Q_{nm}^T + \frac{16}{L_x L_y (1 - v_{PZT})} (h_T + h_{PZT}) E_{PZT} d_{31} V \left[\left(\frac{m}{L_x} \right)^2 \right. \\
& + \left. \left(\frac{n}{L_y} \right)^2 \right] \sin \frac{m\pi}{2} \sin \frac{m\pi}{2L_x} \sin \frac{n\pi}{2} \sin \frac{n\pi}{2L_y} \quad (17)
\end{aligned}$$

where the generalized random forces Q_{nm}^T are

$$Q_{nm}^T(t) = \frac{\int_0^{L_x} \int_0^{L_y} P_T(x, y, t) X_{nm}(x, y) dx dy}{\int_0^{L_x} \int_0^{L_y} X_{nm}^2(x, y) dx dy} \quad (18)$$

The operator $\langle \Omega_T, f \rangle$ denotes the integration

$$\langle \Omega_T, f \rangle = \int_0^{L_y} \int_0^{L_x} \Omega_T f dx dy \quad (19)$$

and $Z_{nmijklrs}$, $\bar{\alpha}$, and $\bar{\gamma}$ are given in the Appendix. A similar equation to that given in Eq. (17) can be developed for the bottom plate. For the cases of five and nine piezoelectric actuators bonded to the face plates, the control forces are given in Ref. 33.

The system of nonlinear coupled differential equations of the top [Eq. (17)] and bottom plates can now be solved by standard numerical integration routines that are available for solution of differential equations. Then, from the response time histories, rms values, probability density histograms, peak distributions, crossing rates, and spectral densities can be estimated. The spectral densities are calculated utilizing the FFT algorithm.

The generalized random forces in Eq. (18) can be obtained by either simulating Q_{nm}^T as a multivariate random process,²⁹ or first simulating pressure $P_T(x, y, t)$ and then evaluating the integrals in Eq. (18) numerically. In the present study, the random pressure is assumed to be stationary, Gaussian, and uniformly distributed over the top plate surface. Then, the generalized random forces can be obtained from

$$\begin{aligned}
Q_{nm}^T(t) &= \frac{16}{mn\pi^2} P_T(t) \quad m, n \text{ odd} \\
&= 0 \quad \text{otherwise}
\end{aligned} \quad (20)$$

where $P_T(t)$ can be simulated as²⁹

$$P_R(t_k) = \text{Re} \left\{ \sum_{s=0}^{M-1} [2S_P(\omega_s) \Delta\omega]^{1/2} \exp[-i(\omega_s t_k + \varsigma_s)] \right\} \quad (21)$$

where Re indicates the real part, $S_P(\omega_s)$ is the pressure input spectral density, ω_s are the frequencies at which values of spectral density are selected, ς_s are the random phase angles uniformly distributed between 0 and 2π , $t_j = j\Delta t$ are discrete time points at which the random pressure is simulated with $j = 0, 1, \dots, M-1$, and time increment

$$\Delta t = 2\pi/\Delta\omega M \quad (22)$$

The frequency bandwidth $\Delta\omega$ can be selected from

$$\Delta\omega = (\omega_u - \omega_l)/N \quad (23)$$

in which ω_u and ω_l denote the upper and lower cutoff frequencies of spectral density $S_P(\omega)$, respectively, and N is the number of spectral density divisions. The FFT algorithm can be applied directly to Eq. (20), where $M = 2^m$ is the number of simulated points.

A simple and very convenient form of spectral density $S_P(\omega)$ is the band-limited Gaussian white noise. Then, S_P can be expressed in terms of sound pressure levels (SPL) in units of decibels (dB) as

$$\begin{aligned}
S_P(\omega) &= \frac{p_0^2}{\Delta\omega} 10^{\text{SPL}/10} \quad \omega_l \leq \omega \leq \omega_u \\
&= 0 \quad \text{otherwise}
\end{aligned} \quad (24)$$

where p_0 is the reference pressure ($p_0 = 2.0 \times 10^{-5} \text{ N/m}^2$).

Noise Transmission

Consider noise transmission through a double-wall sandwich construction into a rectangular enclosure that occupies a volume $V_e = abd$ (Fig. 1). Except for the double-wall panel, the remaining walls are assumed to be rigid. The perturbation pressure inside the enclosure can be determined from the linear acoustic wave equation

$$\nabla^2 p - \mu \dot{p} = \frac{1}{c_0^2} \ddot{p} \quad (25)$$

where $\nabla^2 = \partial^2/\partial x^2 + \partial^2/\partial y^2 + \partial^2/\partial z^2$, μ is the acoustic damping, and the boundary conditions that express continuity of normal velocity between fluid and the walls are

$$\frac{\partial p}{\partial n} = 0 \quad \text{on rigid boundary} \quad (26)$$

$$\frac{\partial p}{\partial n} = -\rho_a \ddot{w}_B \quad \text{on flexible boundary} \quad (27)$$

where n denotes the outward normal to the wall surface, and w_B is the displacement of the bottom plate in the z direction.

Equations (25–27) form a set of homogeneous equations with nonhomogeneous time-dependent boundary conditions. The homogeneous equation with nonhomogeneous boundary conditions can be transformed into a nonhomogeneous equation with homogeneous boundary conditions by setting^{34,35}

$$p(x, y, z, t) = q(x, y, z, t) + \rho_a \ddot{w}_B G(z) \quad (28)$$

where the function $G(z)$ is chosen to satisfy the given boundary conditions, and q is the solution of the associated boundary value problem. The function $G(z)$ can be chosen as

$$G(z) = z - (z^2/2b) \quad (29)$$

The solution for q has been developed in Ref. 34, using acoustic modes of a hard-wall cavity. Then, taking the Fourier transformation of Eqs. (25–28) and using the random process the-

ory,³⁶ the spectral density $S_P(x, y, z, \omega)$ of the interior acoustic pressure can be determined. This spectral density is a function of structural vibration response of the double-wall system. By reducing structural vibrations, noise transmission into the enclosure can be reduced. However, for linear cases where acoustic modes dominate transmitted noise, the velocity feedback approach might not provide the required noise attenuation.^{11,13,14,28} For the nonlinear vibrations considered in this study, the coupling mechanism between structural vibrations and interior acoustic pressure is different, because all of the structural modes are coupled and it is not possible to identify distinct structural modes that are strongly coupled to specific acoustic modes.

Numerical Results

The material and geometric parameters selected in this study correspond to a typical double-wall construction that could represent a local component of the thermal surface protection system of flight structures. Because of a requirement of significant computation time for simulation and the integration of nonlinear equations of motion, numerical results are aimed mainly at illustrating the feasibility of using a PZT-based velocity feedback mechanism for the control of nonlinear vibrations and noise transmission. Furthermore, results are presented for aluminum face plates of the double-wall construction. Other materials, including fiber-reinforced composites, could easily be accommodated in the present approach.⁸

Numerical results are presented for the following parameters of the double-wall panel and acoustic enclosure: $a = 0.6096$ m, $b = 0.9144$ m, $d = 0.9144$ m, $L_x = 0.2032$ m, $L_y = 0.3048$ m, $E_T = E_B = 6.89 \times 10^{10}$ N/m², $\rho_T = \rho_B = 273.52$ kg-s²/m⁴, $\nu_T = \nu_B = 0.3$, $h_T = h_B = 0.001016$ m, $h_S = 0.0254$ m, $\rho_S = 12.4$ kg-s²/m⁴, $c_0 = 344$ m/s, $k_1 = 5.4289 \times 10^5$ N/m³, $k_2 = k_3 = 0$, $c_1 = c_2 = c_3 = 0$. Numerical results were also obtained for $k_1 = 5.4289 \times 10^6$ N/m³, $k_2 = 0$, $k_3 = 4.2074 \times 10^{10}$ N/m⁵. The geometric and material properties of piezoelectric sensors/actuators are $A = 0.0127$ m, $B = 0.0635$ m, $h_{PZT} = 2.5 \times 10^{-4}$ m, $E_{PZT} = 6.89 \times 10^{10}$ N/m², $\nu_{PZT} = 0.3$, $\rho_{PZT} = 273.52$ kg-s²/m⁴, $d_{31} = d_{32} = 2 \times 10^{-10}$ m/V.

The modal structural and modal acoustic damping were taken as

$$\xi_{mi} = \xi_{11}(\omega_{11}/\omega_{mi}) \quad (30)$$

$$\Phi_{ijk} = \mu c_0^2 / 2\omega_{ijk} = \xi_0(\omega_1/\omega_{ijk}) \quad (31)$$

in which ξ_{11} , ξ_0 are selected damping coefficients, ω_1 is the lowest acoustic modal frequency inside the enclosure, and ω_{ijk} are hard-wall acoustic modal frequencies of the rectangular enclosure shown in Fig. 1. The results represented here are for $\xi_{11} = 0.02$, $\xi_0 = 0.05$. In this approach, the effects of radiation damping and absorption at the walls in the interior of the cavity are represented by equivalent modal damping Φ_{ijk} . Noise reduction (NR) for the double-wall panel system is defined as

$$NR(x, y, z, \omega) = 10 \log_{10} \frac{S_P(\omega)}{S_P(x, y, z, \omega)} \quad (32)$$

where $S_P(\omega)$ is the spectral density of the uniformly distributed input random pressure acting on the top plate.

The random pressure $P_T(t)$ was simulated using $\omega_1 = 0$, $\omega_u = 2\pi \times 500$ rad/s, $N = 512$, $M = 4096$, and several different values of SPL.

The velocity feedback control with piezoelectric actuators is to set the output voltage of the actuators proportional to the modal velocities. In the present study, the dominant plate modes for the frequency range of 0–500 Hz are (1, 1), (1, 2),

and (1, 3). Then, for a single actuator placed in the middle of the plate, the applied voltage in Eq. (17) can be set as

$$V(t) = -K(\dot{A}_{11}^T - \dot{A}_{13}^T) \quad (33)$$

To avoid the depoling effect and possible nonlinear behavior of the electromechanical relations, the factor K should not exceed a value for which the piezoelectric actuator would not function properly for the applied voltage.²⁸

Structural Response

The controlled and noncontrolled response time histories of the bottom plate are presented in Figs. 3 and 4. These deflections correspond to the middle of the plate. For SPL = 80 dB, the response is linear, whereas for SPL = 120 dB, it is nonlinear. For the selected geometry of the double-wall panel, nonlinear effects start to influence structural response for input SPL exceeding 100 dB. As can be seen from these results, active velocity feedback control could be very effective in reducing linear and nonlinear vibrations. For nonlinear cases, active control not only reduces vibration amplitudes but also has an effect on shifting dominant vibration frequencies to lower values. The rms response vs the rms input pressure is given in Fig. 5 for several arrangements of piezoelectric actuators and voltage gains, $K = 0$ and 393.7 V-s/m. Significant reduction in vibrations of both top and bottom plates can be achieved with a single actuator placed at the middle of either the top or bottom plate. A larger number of actuators further reduces vibration response. However, the incremental gains of nonlinear response reduction tend to decrease as more PZT actuators are added to the double-wall panel.

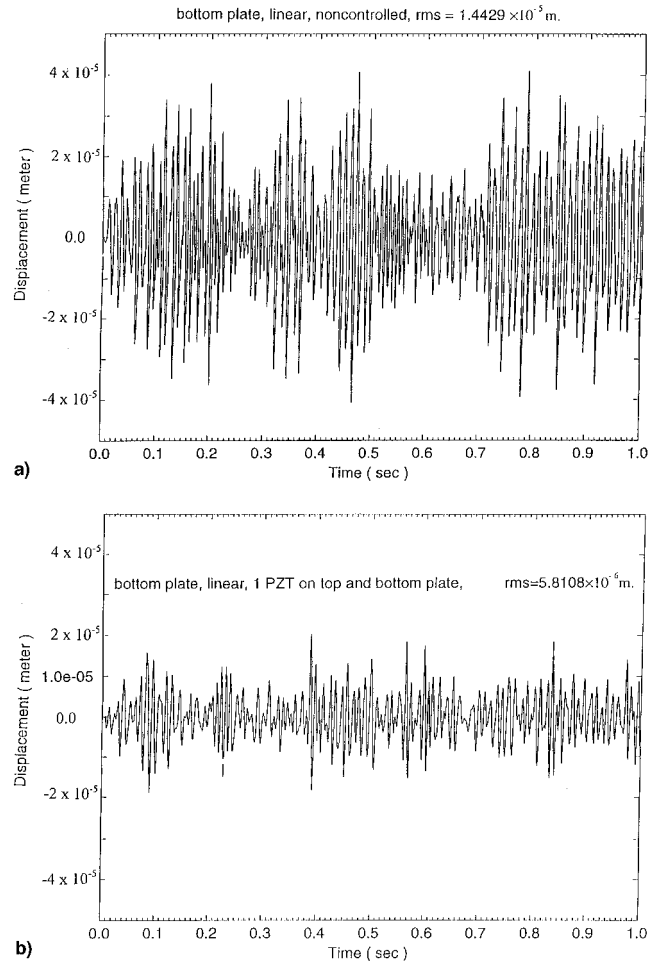


Fig. 3 Displacement response time history of bottom plate a) without and b) with active control (SPL = 80 dB).

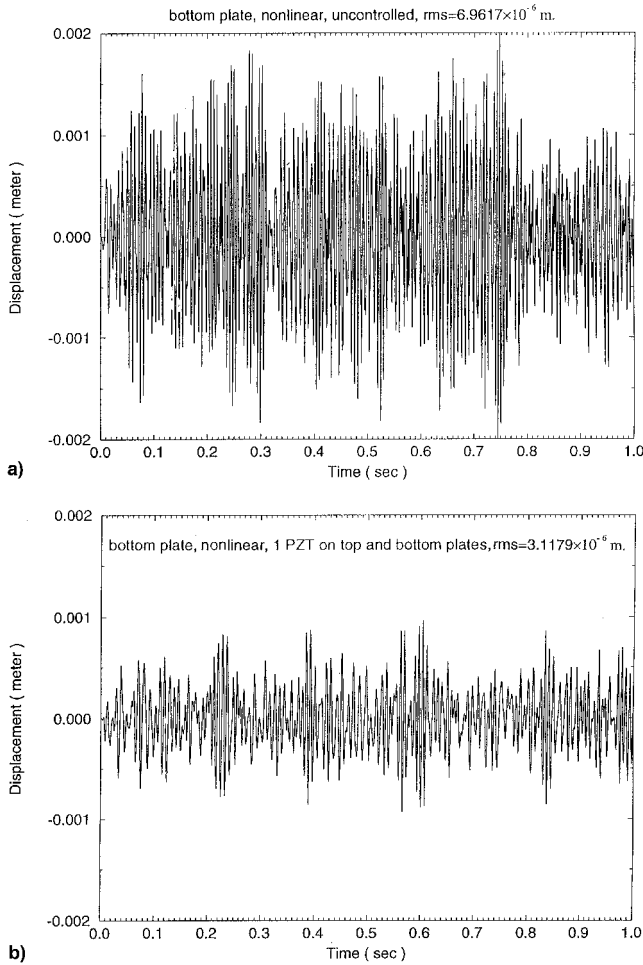


Fig. 4 Displacement response time history of bottom plate a) without and b) with active control (SPL = 120 dB).

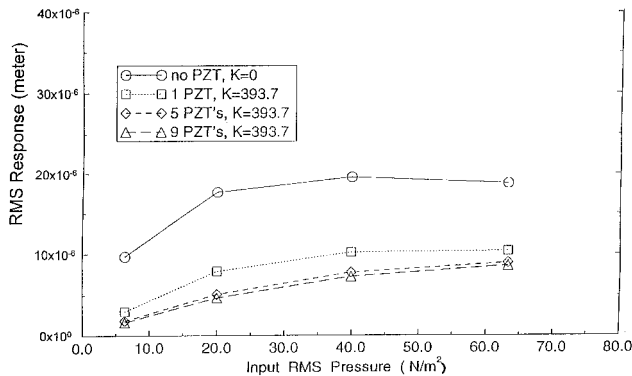


Fig. 5 Root-mean-square response of top plate for different arrangement of PZT actuators.

The response spectral densities for linear and nonlinear vibrations are presented in Figs. 6 and 7 for the case of a single sensor/actuator. For linear vibrations, the distinct peaks associated with flexural and dilational modes are clearly evident in Fig. 6. However, for the nonlinear case, the spectral densities tend to exhibit a broadband character with dominant peaks shifted to higher frequency values. Furthermore, active vibration control reduces panel response and the effect of nonlinearity on structural vibrations. Thus, dominant vibration peaks tend to shift back to lower frequency values. The linear vibrations by the time-domain approach given in Fig. 6 were verified by a closed-form solution using the spectral density method.

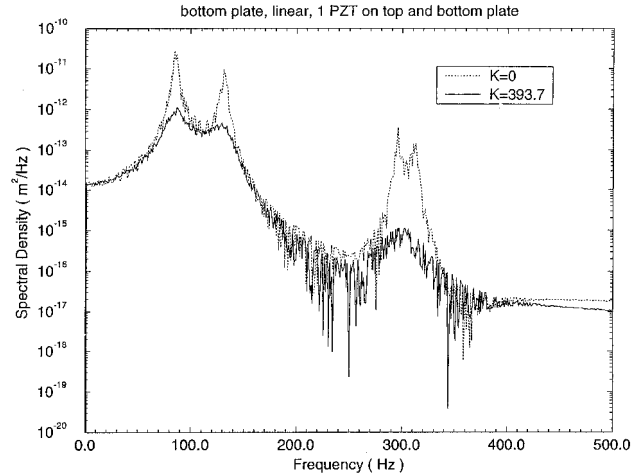


Fig. 6 Displacement response spectral density for input SPL = 80 dB.

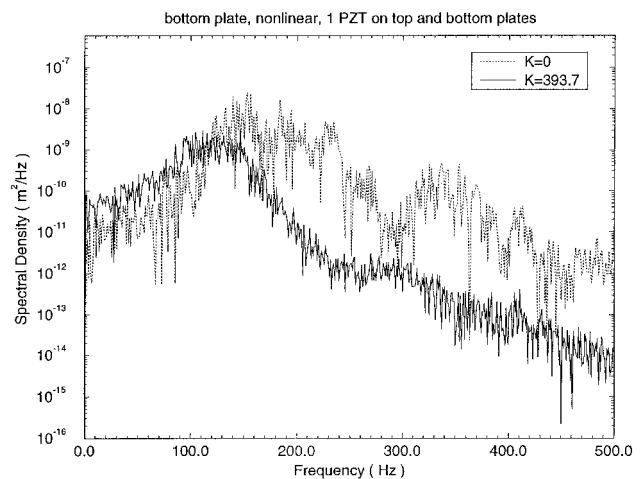


Fig. 7 Displacement response spectral density for input SPL = 120 dB.

The nonlinear terms from stretching of the plate tend to reduce the effectiveness of the velocity feedback control. This is because when the maximum amplitude of nonlinear vibrations reaches a level where both surfaces of each plate are in tension, a pair of PZT actuators inducing a local bending moment are less effective than for a case of linear response where one side of the plate is in tension and the other side is in compression. In addition, for nonlinear vibrations, the modes could become strongly coupled and the velocity feedback control mechanism that was optimized for a set of dominant modes of linear response might not achieve the required objective.

Numerical results were also obtained for different linear and nonlinear stiffness values of the elastic soft core. For a stiff core with $k_1 = 5.4289 \times 10^6 \text{ N/m}^3$ and $k_2 = k_3 = 0$, the response of top and bottom plates is almost the same, whereas for a softer core with $k_1 = 5.4289 \times 10^5 \text{ N/m}^3$, nonlinear vibrations of the bottom plate are about 50% lower than those of the top plate. A similar trend was observed when the core stiffness was modeled by nonlinear springs. For $k_3 = 4.2074 \times 10^{10} \text{ N/m}^5$, vibrations of both plates are almost the same. However, for k_3 values below $1.6830 \times 10^{10} \text{ N/m}^5$, nonlinear vibrations of the bottom plate are about one half in magnitude to those of the top plate when the input sound pressure reaches 120 dB. Thus, the design of the active vibration control system for double-wall sandwich panels requires not only properties of the core material but also information on the linear/nonlinear behavior of the core material for different sound pressure input levels.

Noise Transmission

Noise reduction of a double-wall system computed $x = 0.3048$ m, $y = 0.4573$ m, and $z = 0.6096$ m is presented in Figs. 8–10. Note that for a linear analysis, noise reduction is identical for different sound pressure input levels. However, for nonlinear vibrations, noise reduction is a function of SPL that is acting on the top plate. The results presented in Figs. 8–10 clearly indicate that noise transmission that is dominated by structural responses can be significantly reduced by active velocity feedback control. However, active velocity feedback control is not effective in reducing transmitted noise at the frequencies of acoustic resonances. When the acoustic and structural resonances coincide (Fig. 10), velocity feedback control may provide a substantial noise attenuation at these resonances.

The numerical results presented in this paper and in Ref. 33 indicate that a large number of parameters could influence active control of nonlinear vibrations and noise transmission. Because of the nonlinear plate terms and/or nonlinear behavior of the soft core, it is difficult to develop specific parametric guidelines on the design of a PZT-based velocity feedback active control system. In addition to the options of size, number, and location of PZT actuators, selections for the active control of top, bottom, or both plates need to be evaluated. The coupled frequencies of nonlinear vibrations of a double-wall system are functions of random input pressure level. Thus, it is not meaningful to develop scaling factors that involve ratios of structural/acoustic frequencies and structural–acoustic modal coupling. However, from the results presented in this study and in Ref. 33, some basic trends in the active control of nonlinear vibrations and noise transmission can be established.

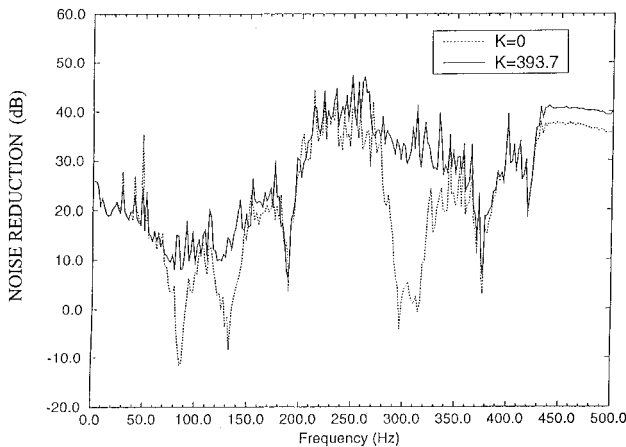


Fig. 8 Noise reduction for input SPL = 80 dB.

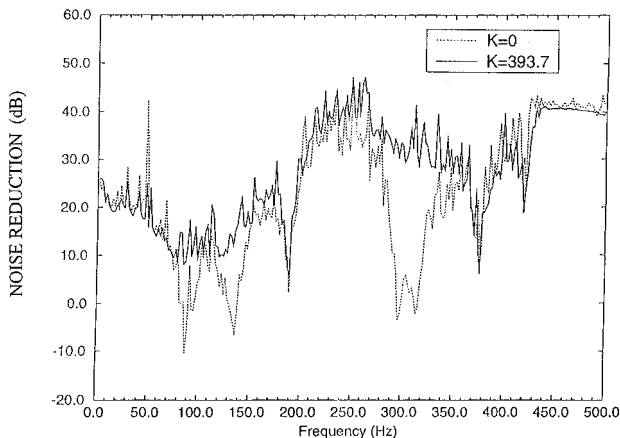


Fig. 9 Noise reduction for input SPL = 100 dB.

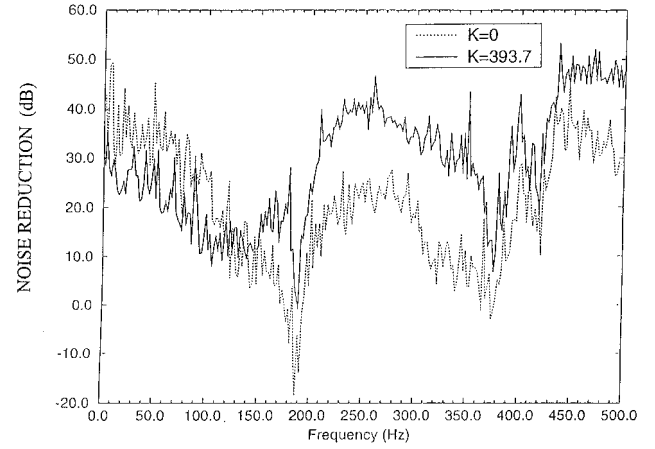


Fig. 10 Noise reduction for input SPL = 120 dB.

The PZT actuators installed on the top and bottom plates are the most effective arrangement to reduce vibrations and noise transmission. If only one plate is used for active control, piezoelectric actuators installed on the top plate provide better results than those installed on the bottom plate. This is because the reduction of nonlinear response of the plate, which is being forced by random pressure, tends to reduce the effect of nonlinear vibration coupling to the other plate. A larger number of actuators and/or larger actuating areas indicate a better performance for vibration and noise transmission reduction. A controller with a large voltage gain factor K seems to be very effective in reducing nonlinear vibrations over the entire frequency range considered in this study. However, it should be noted that a controller with a large gain factor might be difficult to implement.^{12–14,24,25} Because the limit of applied voltage is an important factor for the implementation of piezoelectric actuators, proper selection of size and number of actuators not only improves the efficiency of active control but also provides an alternative to control nonlinear vibrations for the same applied voltage.

Concluding Remarks

This paper presents an analytical model on active control of nonlinear vibrations and noise transmission of double-wall panel systems to wideband random inputs. From the results obtained, the following concluding remarks are made. The velocity feedback control could provide a significant reduction of linear and nonlinear vibrations for both top and bottom plates; higher values of conversion/gain factor, larger size, and larger number of piezoelectric actuators indicate positive gains for vibration control; stiffness nonlinearity of the soft core could have an effect on structural vibrations and noise transmission; substantial noise attenuation can be achieved by active velocity feedback control when the transmitted noise is dominated by structural resonances; velocity feedback control might not be effective where acoustic resonances dominate interior noise; even though the mechanism of nonlinear vibrations is different from that of linear cases, active vibration control technology developed for linear structures could be accommodated to control nonlinear vibrations and noise transmission.

Appendix: Piezoelectric Constants and Nonlinear Coefficients

The matrix $[c_{PZT}]$ is

$$[c_{PZT}] = \frac{E_{PZT}}{1 - \nu_{PZT}^2} \begin{bmatrix} 1 & \nu_{PZT} & 0 \\ \nu_{PZT} & 1 & 0 \\ 0 & 0 & \frac{(1 - \nu_{PZT})}{2} \end{bmatrix} \quad (A1)$$

The terms $\bar{\alpha}$, $\bar{\gamma}$, and $Z_{mnijklrs}$ used in Eq. (17) are

$$\bar{\alpha}(m, i, k) = \alpha(m - i, k) - \alpha(m + i, k) \quad (A2)$$

where

$$\begin{aligned} \alpha(k, l) &= 0 \\ &\text{if } (k + l) \text{ even and } (l - k) \text{ even} \\ \alpha(k, l) &= \frac{1}{(k + l)\pi} + \frac{1}{(l - k)\pi} \\ &\text{if } (k + l) \text{ odd and } (l - k) \text{ odd} \\ \alpha(k, l) &= \frac{1}{(k + l)\pi} \\ &\text{if } (k + l) \text{ odd and } (l - k) \text{ even} \\ \alpha(k, l) &= \frac{1}{(l - k)\pi} \\ &\text{if } (k + l) \text{ even and } (l - k) \text{ odd} \end{aligned} \quad (A3)$$

$$\begin{aligned} \bar{\gamma}(m, i, k, r) &= \gamma(m - i, k - r) - \gamma(m + i, k - r) \\ &- \gamma(m - i, k + r) + \gamma(m + i, k + r) \end{aligned} \quad (A4)$$

where

$$\begin{aligned} \gamma(m, n) &= 2 \quad \text{if } m = n = 0 \\ \gamma(m, n) &= 1 \quad \text{if } m = |n| \neq 0 \\ \gamma(m, n) &= 0 \quad \text{otherwise} \end{aligned} \quad (A5)$$

$$\begin{aligned} Z_{mnijklrs} &= ks(lr - ks)[F_{mnijklrs}(k + r, l + s) \\ &+ \bar{F}_{mnijklrs}(k - r, l - s)] + ks(lr + ks)[F_{mnijklrs}(k - r, l + s) \\ &+ F_{mnijklrs}(k + r, l + s)] \end{aligned} \quad (A6)$$

where

$$\begin{aligned} F_{mnijklrs}(G, H) &= \{2GHij[\beta(m + i, G) \\ &+ \beta(m - i, G)][\beta(n + j, H) + \beta(n - j, H)] \\ &- (H^2k^2 + G^2l^2)[\gamma(m + i, G) - \gamma(m - i, G)][\gamma(n + j, H) \\ &- \gamma(n - j, H)]\}/[G^2 + H^2(L_y/L_x)^2] \end{aligned} \quad (A7)$$

$$\begin{aligned} \bar{F}_{mnijklrs}(G, H) &= 0 \quad \text{if } G = H = 0 \\ \bar{F}_{mnijklrs}(G, H) &= F_{mnijklrs}(G, H) \quad \text{otherwise} \end{aligned} \quad (A8)$$

with

$$\begin{aligned} \beta(p, q) &= 1 \quad \text{if } p = q \neq 0 \\ \beta(p, q) &= -1 \quad \text{if } p = -q \neq 0 \\ \beta(p, q) &= 0 \quad \text{otherwise} \end{aligned} \quad (A9)$$

References

- ¹Pozefsky, P., and Blevins, R. D., "Thermo-Vibro-Acoustic Loads and Fatigue of Hypersonic Flight Vehicle Structure," Air Force Wright Aeronautical Lab., TR-89-3014, Wright-Patterson AFB, OH, 1989.
- ²Cazier, F. W., Jr., Dogget, V., Jr., and Rickett, R. H., "Structural Dynamic and Aeroelastic Considerations for Hypersonic Vehicles," AIAA Paper 91-1225, April 1991.
- ³Vaicaitis, R., "Nonlinear Response and Sonic Fatigue of National Aerospace Space Plane Surface Panels," *Journal of Aircraft*, Vol. 31, No. 1, 1994, pp. 10-18.
- ⁴Vaicaitis, R., Dowell, E. H., and Ventres, C. S., "Nonlinear Panel Response by a Monte Carlo Approach," *AIAA Journal*, Vol. 12, No. 5, 1974, pp. 685-691.
- ⁵Hong, H.-K., and Vaicaitis, R., "Nonlinear Response of Double Wall Sandwich Panels," *Journal of Structural Mechanics*, Vol. 12, No. 4, 1984, pp. 483-503.
- ⁶Choi, S. T., and Vaicaitis, R., "Nonlinear Response and Fatigue of Stiffened Panels," *Probabilistic Engineering Mechanics*, Vol. 4, No. 3, 1989, pp. 150-160.
- ⁷Mei, C., and Paul, D. B., "Nonlinear Multimode Response of Clamped Rectangular Plates to Acoustic Loading," *AIAA Journal*, Vol. 24, No. 4, 1986, pp. 643-648.
- ⁸Kavallieratos, P., and Vaicaitis, R., "Nonlinear Response of Composite Panels of High Speed Aircraft," *Composite Engineering*, Vol. 3, Nos. 7, 8, 1993, pp. 645-660.
- ⁹Lee, J., "Large-Amplitude Plate Vibration in an Elevated Thermal Environment," *Applied Mechanics Reviews*, Vol. 46, No. 11, Pt. 2, 1993.
- ¹⁰Fuller, C. R., Rogers, C. A., and Robertshaw, H. H., "Control of Sound Radiation with Active/Adaptive Structures," *Journal of Sound and Vibration*, Vol. 157, No. 1, 1992, pp. 19-39.
- ¹¹Koshigoe, S., and Murdock, J. W., "A Unified Analysis of Both Active and Passive Damping of a Plate with Piezoelectric Transducers," *Journal of the Acoustical Society of America*, Vol. 93, No. 1, 1993, pp. 346-355.
- ¹²Kim, S. J., and Jones, J. D., "Optimal Design of Piezoactuators for Active Noise and Vibration Control," *AIAA Journal*, Vol. 29, No. 12, 1991, pp. 944-951.
- ¹³Crawley, E. F., and Lazarus, K. B., "Induced Strain Actuation of Isotropic and Anisotropic Plates," *AIAA Journal*, Vol. 29, No. 6, 1991, pp. 944-951.
- ¹⁴Tzou, H. S., and Fu, H. Q., "A Study of Segmentation of Distributed Piezoelectric Sensors and Actuators, Part I: Theoretical Analysis," *Journal of Sound and Vibration*, Vol. 172, No. 2, 1994, pp. 247-259.
- ¹⁵Pan, J., Hansen, C. H., and Bies, D. A., "Active Control of Noise Transmission Through a Panel into a Cavity, Part I: Analytical Study," *Journal of the Acoustical Society of America*, Vol. 87, No. 5, 1990, pp. 2098-2108.
- ¹⁶Jones, J. D., and Fuller, C. R., "Active Control of Sound Fields in Elastic Cylinders by Multicontrol Forces," *AIAA Journal*, Vol. 27, No. 7, 1989, pp. 845-852.
- ¹⁷Silcox, R. J., Fuller, C. R., and Lester, H. C., "Mechanisms of Active Control in Cylindrical Fuselage Structures," *AIAA Journal*, Vol. 28, No. 8, 1990, pp. 1397-1404.
- ¹⁸Koshigoe, S., Gillis, J. R., and Falangas, E. T., "A New Approach for Active Control of Sound Transmission Through an Elastic Plate Backed by a Rectangular Cavity," *Journal of the Acoustical Society of America*, Vol. 94, No. 2, Pt. 1, 1993, pp. 900-907.
- ¹⁹Fuller, C. R., Hansen, C. H., and Snyder, S. D., "Active Control of Sound Radiation from a Vibrating Rectangular Panel by Sound Sources and Vibration Inputs: An Experimental Comparison," *Journal of Sound and Vibration*, Vol. 145, No. 2, 1991, pp. 195-215.
- ²⁰Snyder, S. D., and Hansen, C. H., "Mechanisms of Active Noise Control by Vibration Sources," *Journal of Sound and Vibration*, Vol. 147, No. 3, 1991, pp. 519-525.
- ²¹Batchellor, C. R., Darkin, J. P., and Pearce, D. A. J., "Fiber Optic Mechanical Sensors for Aerospace Applications," *International Journal of Optic Sensors*, Vol. 2, Nos. 5, 6, 1987, pp. 407-411.
- ²²Rogers, C. A., Liang, C., and Barker, D. K., "Dynamic Control Concepts Using Shape Memory Alloy Reinforced Plates," *Smart Materials, Structures and Mathematical Issues*, edited by C. A. Rogers, Technomic, Westport, CT, 1989.
- ²³Baz, A., Inman, K., and McCoy, J., "Active Control of Flexible Beams Using Shape Memory Actuators," *Journal of Sound and Vibration*, Vol. 140, No. 3, 1990, pp. 437-456.
- ²⁴Uchino, K., "Electrostrictive Actuators: Materials and Applications," *American Ceramic Society Bulletin*, Vol. 65, April 1986, pp. 647-652.
- ²⁵Butler, J. L., *Application Manual for the Design of ETREMA Tefenol-D Magnetostrictive Transducers*, Edge Technologies, Inc., 1988.
- ²⁶Randall, R. J., and Tsang, W. F., "Use of Electro-Rheological Fluids for Adaptive Vibration Isolation," 1st European Conf. on Smart Materials, European Optical Society, Glasgow, 1992.
- ²⁷Chia, C.-Y., *Nonlinear Analysis of Plates*, McGraw-Hill, New York, 1980.
- ²⁸Lee, C. K., "Theory of Laminated Piezoelectric Plates for the Design of Distributed Sensors/Actuators, Part I: Governing Equations and Reciprocal Relationships," *Journal of the Acoustical Society of America*, Vol. 87, No. 3, 1990, pp. 1144-1158.

- ²²Shinozuka, M., and Jan, C.-M., "Digital Simulation of Random Processes and Its Applications," *Journal of Sound and Vibration*, Vol. 25, No. 1, 1972, pp. 111–128.
- ²³Bolotin, V. V., *Nonconservative Problems of the Theory of Elastic Stability*, Pergamon, Oxford, England, UK, 1963.
- ²⁴Dowell, E. H., "Transmission of Noise from a Turbulent Boundary Layer Through a Flexible Plate into a Closed Cavity," *Journal of the Acoustical Society of America*, Vol. 46, No. 1, 1969, pp. 238–252.
- ²⁵"ANSI/IEEE Standard 176," *Piezoelectricity*, Inst. of Electrical and Electronics Engineers, New York, 1987.
- ²⁶Wei, Y., "Active Vibration and Noise Transmission Control of Nonlinear Double Wall Panel Systems," Ph.D. Dissertation, Dept. of Civil Engineering and Engineering Mechanics, Columbia Univ., New York, Aug. 1995.
- ²⁷McDonald, W. B., Vaicaitis, R., and Myers, M. K., "Noise Transmission Through Plate into an Enclosure," NASA TP 1173, May 1978.
- ²⁸Courant, R., and Hilbert, D., *Methods of Mathematical Physics*, Vol. 1, Interscience, New York, 1953.
- ²⁹Lin, Y. K., *Probabilistic Theory of Structural Dynamics*, McGraw-Hill, New York, 1967; reprint, Krieger, Melbourne, FL, 1976.